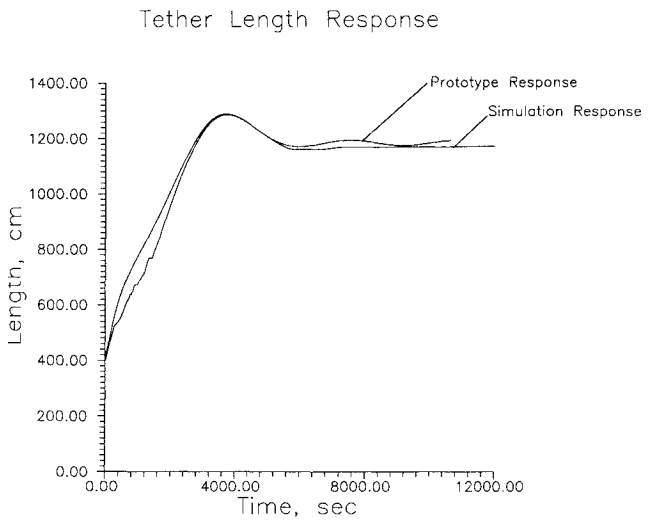

Fig. 4 Length response vs time for a 12-m deployment using the trajectory method.

results for the differencing method, while Fig. 4 shows the trajectory method results. Both methods produce tether length profiles comparable to simulation results. Maximum deployed length errors in both tests were approximately 8% for the trajectory method and less than 0.8% for the differencing method. Although the magnitude of either length error might be considered acceptable, the differencing method is clearly superior.

Conclusions

The results reported here indicate that the prototype reel mechanism performs satisfactorily compared to simulations. The demonstrated deployment and retrieval rates also appear adequate for a space-based system. Additionally, length errors were within acceptable limits and the yo-yo damping scheme has been shown successful.

Acknowledgment

This work was supported in part by a grant from NASA Marshall Space Flight Center, Alabama.

References

[1]Greene, M., Rupp, C. C., Walls, J., Wheelock, D., and Lorenzoni, A., "Feasibility Assessment of the Getaway Tether Experiment," *The Journal of the Astronautical Society,* Vol. 35, No. 1, 1987, pp. 97–118.

[2]Deloach, R., Wood, G., Rupp, C., Harrison, J., and Crumbly, K., "Tethered Dynamics Explorer and Tethered Atmospheric Probe: A Low-Cost, Low-Risk Tethered Satellite Flight Program," *Proceedings of the Third International Conference on Tethers in Space-Toward Flight,* Vol. CP 892, AIAA, Washington, DC, 1989, pp. 115–118.

[3]Greene, M., Gwaltney, D., Stover, G., Kromann, D., and Walls, J., "Getaway Tether Experiment (GATE) for the Tether Dynamics Explorer (TDE) Series," *Proceedings of the Third International Conference on Tethers in Space-Toward Flight,* Vol. CP 892, AIAA, Washington, DC, 1989, pp. 33–40.

[4]Rupp, C. C., "A Tether Tension Control Law for Tethered Satellites Deployed Along the Local Vertical," NASA TMS-6493, Marshall Space Flight Center, AL, Sept. 1975.

[5]Baker, W. P., Dunkin, J. A., Galaboff, Z. J., Johnston, D. D., Kissel, R., Rheinfurth, M. H., and Siebel, M. P. L., "Tethered Subsatellite Study," NASA TMX-73314, Marshall Space Flight Center, AL, March 1976.

[6]Modi, V. J., and Misra, A. K., "On the Deployment Dynamics of Tether Connected Two-Body Systems," *Acta Astronautica,* Vol. 6, No. 9, 1979, pp. 1183–1197.

[7]Davis, W. R., and Banerjee, A. K., "Libration Damping of a Tethered Satellite by Yo-Yo Control with Angle Measurement," *Journal of Guidance, Control, and Dynamics,* Vol. 13, No. 2, 1990, pp. 370–374.

Estimating Damping in Higher Order Dynamic Systems

James W. Banham*
Drexel University, Philadelphia, Pennsylvania 19104

Introduction

THOSE whose activities in engineering practice bring them into contact with dynamic systems are often concerned with determining the amount of damping present in a particular system. A common example is that of the control systems engineer tuning the forward path gain of a feedback control loop to optimize the transient response of one or more variables in the loop. Another is the experimental determination of modal damping coefficients of flexible systems. Existing experimental methods for obtaining quantitative damping data are lengthy and often require the introduction of unacceptable disturbances into the system.

This Note shows how finding just two points on a Bode diagram phase angle curve can, with remarkable accuracy, pinpoint the damping ratio of any system characterized by a dominant pair of complex poles. The experimental equipment required consists of a signal generator, a dual channel oscilloscope, and suitable transducers and other interface instrumentation. The procedure is straightforward and requires a minimum of supporting analysis.

Systems containing static and dynamic nonlinearities exhibit an approximate linear response when excited by small amplitude disturbances.[1] This allows such systems to be tested according to the method and their damping characteristics specified in approximate terms as a linear damping ratio, thus extending the utility of the method to many real systems.

Second-Order System

The frequency response of a second-order system is highly dependent on its damping ratio.[2] The classical family of Bode magnitude and phase curves depicted in any standard text on vibrations, dynamic systems, or control theory illustrates this dependency. It is seen that the slope of the phase curve at the point (ω_n, -90 deg) varies over a wide range from the critically damped ($\zeta=1$) to the undamped ($\zeta=0$). We know that the slope of a first-order system phase curve at the natural frequency ω_n is -66 deg/decade,[3] giving twice that value, or -132 deg/decade, for a critically damped second-order system at the undamped natural frequency. This slope becomes increasingly negative as damping is reduced, approaching infinity as all damping vanishes. The slope is thus seen to be a sensitive indicator of the amount of damping present, and a quantitative correlation of the slope with the damping ratio will allow the estimation of damping in real systems, both second order and those with a single pair of dominant complex poles.

Phase Angle Slope

The generalized second-order system transfer function

$$G(s)=\frac{\omega_n^2}{s^2+2\zeta\omega_n s+\omega_n^2} \tag{1}$$

transforms to the frequency transfer function

$$G(j\omega)=\frac{\omega_n^4-\omega_n\omega^2-j(2\zeta\omega_n^3\omega)}{\omega_n^4+(4\zeta^2-2)\omega_n^2\omega^2+\omega^4} \tag{2}$$

Received Nov. 2, 1990; revision received Feb. 14, 1991; accepted for publication Feb. 25, 1991.

*University Lecturer and Associate Department Head, Department of Mechanical Engineering and Mechanics.

for which the phase angle is

$$\phi = \angle G(j\omega) = \tan^{-1}\frac{\mathrm{Im}\{G(j\omega)\}}{\mathrm{Re}\{G(j\omega)\}} = \tan^{-1}\frac{-2\zeta\omega_n\omega}{\omega_n^2-\omega^2} \tag{3}$$

It is noted here that at $\omega=\omega_n$, i.e., resonance,

$$\phi = \angle G(j\omega_n) = -90 \text{ deg} \tag{4}$$

and it is at this precise point where we wish to find the slope of the phase angle curve. To simplify the system, we normalize the frequency by letting $\bar{\omega}=\omega/\omega_n$ and differentiate the result with respect to frequency. This produces

$$\frac{d\phi}{d\omega} = \frac{-2\zeta(\bar{\omega}^2+1)}{\left[\bar{\omega}^4+2(2\zeta^2-1)\bar{\omega}^2+1\right]\omega_n} \tag{5}$$

the slope of the phase angle curve as a function of the normalized frequency. To find this slope at the undamped natural frequency ω_n in units of radians per radian per second, let $\bar{\omega}=1$ in Eq. (5), giving the phase curve slope

$$\frac{d\phi}{d\omega} = -\frac{1}{\zeta\omega_n} \tag{6}$$

so at $\omega=\omega_n$

$$\frac{d\phi}{df} = \frac{d\phi}{d\omega}\frac{d\omega}{df} = -\frac{2\pi}{\zeta\omega_n} \text{ rad/Hz} = -\frac{360}{\zeta\omega_n} \text{ deg/Hz} \tag{7}$$

where f is the frequency in hertz. The slope of the phase curve at the undamped natural frequency when plotted on the semilogarithmic Bode diagram may be found by making the transformation $\omega^*=\log\omega$. Then,

$$\frac{d\omega^*}{d\omega} = \frac{1}{\ell n 10}\times\frac{1}{\omega} \tag{8}$$

$$\frac{d\phi}{d\omega^*} = \frac{d\phi}{d\omega}\frac{d\omega}{d\omega^*} = \ell n(10)\omega\frac{d\phi}{d\omega} \tag{9}$$

which, when evaluated at $\omega=\omega_n$, is

$$\frac{d\phi}{d\omega^*} = \frac{\ell n 10}{\zeta} = -\frac{2.304}{\zeta} \text{ rad/decade} \tag{10}$$

Equation (10) gives the number of radians change in the tangent for a unit change in ω^*, i.e., over one cycle (or decade) of the logarithmic scale. Converting from radians to degrees,

$$\frac{d\phi}{d\omega^*} = -\frac{2.304}{\zeta}\times\frac{180 \text{ deg}}{\pi \text{ rad}} \tag{11}$$

or its equivalent in the Bode plot phase angle diagram:

$$\frac{d\phi}{d\omega^*} = -\frac{132}{\zeta}\frac{\text{deg}}{\text{decade}} \tag{12}$$

Equation (12) constitutes a useful rule as an aid in sketching the frequency response Bode diagram of an underdamped second-order system.

Feedback Control Example

Consider the case of the unity feedback system with transfer function

$$G(s) = \frac{6800K}{s^5+48s^4+792s^3+4800s^2+6800s} \tag{13}$$

This system is overdamped for low values of the gain K, critically damped at $K\approx 0.4$, and underdamped at higher values of K. This is evident from the root-locus diagram of Fig. 1.

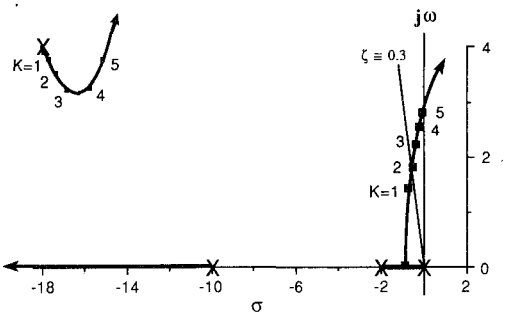

Fig. 1 Root locus of fifth-order system.

Table 1 Fifth-order system phase angle data

f, Hz	ω, rad/s	ϕ, rad	ϕ, deg
0.272	1.708	−1.569	−90.0
0.250	1.571	−1.309	−75.0

Suppose we wish to estimate the damping associated with the dominant poles of the closed-loop system at $K=2$. The following procedure is suggested.[4]

1) With the system operating in the steady state with a constant reference input signal, add a small amplitude sinusoidal input from a harmonic signal generator at a frequency estimated to be in the neighborhood of the dominant natural frequency. (An operational summing amplifier is often used for this purpose.)

2) While observing both the input and output signal on an oscilloscope or pen recorder, adjust the frequency until an output signal phase lag of 90 deg with respect to the input is observed. The amplitude of the input should be no larger than is necessary to permit the observation of a pair of signals reasonable free of noise. Carefully determine and record the exact phase angle. (A digital storage oscilloscope is an excellent instrument for capturing low-frequency signals, such as might be seen in the test of a process control system.) Next, observe and record the frequency (this is the natural frequency f_n).

3) Slowly decrease the frequency until a measurable change in phase angle is observed. Record both the frequency and phase angle.

4) Divide the phase increase by the frequency decrease. This is (the negative of) the approximate slope of the phase angle at the undamped natural frequency, in degrees per hertz. Then multiply this slope by the natural frequency $2\pi f_n$. When the product is divided into 360 deg, the result, as seen in Eq. (9), is numerically equal to the damping ratio.

For the fifth-order example system, the results of the test just described are summarized in Table 1.

Using the rule of Eq. (9), the damping ratio for this system is determined to be

$$\zeta = \frac{-360}{(\Delta\phi/\Delta f)\omega_n} = \frac{-360}{\left[(75-90)/(0.272-0.250)\right](1.708)} = 0.307 \tag{14}$$

A coarse estimate of the damping ratio may also be obtained from the root-locus diagram. Since

$$\zeta = \cos\theta = \cos\left[\tan^{-1}\frac{|\mathrm{Im}\{G(j\omega)\}|}{|\mathrm{Re}\{G(j\omega)\}|}\right] \tag{15}$$

By estimating the magnitudes of the real and imaginary parts from Fig. 1, we obtain

$$\zeta = \cos\left[\tan^{-1}\frac{1.7}{0.5}\right] = 0.28 \tag{16}$$

The exact roots of the closed-loop characteristic at $K = 2$ are at $s = -12.2$, $s = -0.546 \pm j1.804$, and $s = -17.35 \pm j3.550$, and the dominant pair yields the exact damping ratio of 0.282. The small error in the method, primarily attributable to the influence of other modes, may be somewhat reduced by using both forward and backward perturbations around the natural frequency.

The secondary damping contributed by the other pair of complex poles may sometimes be found by a similar procedure, provided that the mode is well separated from all other modes and that the higher frequency signals are sufficiently large to be measurable without noise interference or overly sophisticated instrumentation systems. In this particular example, the real pole at $s = -12.2$ contributes significant change in phase angle in the spectral region dominated by the other complex poles, thus causing the method to fail.

Conclusions

A simple method for estimating the damping that is present in systems dominated by a single pair of complex conjugate poles has been illustrated. The method constitutes an addition to the tool kit of the dynamic systems experimentalist by providing a relatively straightforward means for the quantitative determination of damping by measurement.

Acknowledgments

The author wishes to thank George J. Thaler of the U.S. Naval Postgraduate School and Albert J. Herr of Drexel University for their valuable comments and suggestions.

References

[1]Warwick, K., *Control Systems: An Introduction,* Prentice-Hall, Englewood Cliffs, NJ, 1989, Chap. 2.

[2]Dorf, R. C., *Modern Control Systems,* Addison-Wesley, Reading, MA, 1989, pp. 277–278.

[3]Caldwell, W. I., Coon, G. A., and Zoss, L. M., *Frequency Response for Process Control,* McGraw-Hill, New York, 1959, p. 60.

[4]Raven, F. H., *Automatic Control Engineering,* 3rd ed., McGraw-Hill, New York, 1978, p. 404.

Use of the Work-Energy Rate Principle for Designing Feedback Control Laws

H.-S. Oh,* S. R. Vadali,† and J. L. Junkins‡
Texas A&M University, College Station, Texas 77843

Introduction

IT is often felt that control designers do not exploit the principles of analytical dynamics in designing feedback control laws for physical systems. It is shown here that for a class of physical systems, feedback control laws are naturally obtained from the system dynamics by using the Work-Energy Rate Principle. It will be seen that the method applies to a wide variety of linear/nonlinear and discrete/continuous systems.

One of the powerful methods of designing feedback control laws for nonlinear systems is based on Lyapunov's second stability theorem.[1] Energy-type quadratic functions are usually used[2-6] in the application of the Lyapunov stability theorem. The time derivative of the Lyapunov function is obtained by substituting the system equations to eliminate acceleration terms. This process is often tedious and involves integration by parts for distributed parameter systems such as flexible spacecraft. If the time derivative of the Lyapunov function can be obtained without substituting the equations of motion, then the control design efforts will be reduced drastically. This is the motivation behind this Note. The expression for the rate of change of system energy is formulated using the Virtual Work Principle,[7,8] and two examples are given to show the power of this method.

Work-Energy Rate Principle

When the system is composed of N particles, it is configured by N physical position vectors $\boldsymbol{x}_k$ measured relative to an inertial frame or $n (n \leq 3N)$ generalized coordinates q_i. The coordinate transformations between the physical and the generalized coordinates are given by

$$\boldsymbol{x}_k = \boldsymbol{x}_k(q_1, q_2, \ldots, q_n, t), \qquad (k = 1,2,\ldots,N) \tag{1}$$

and their time derivatives are related by

$$\dot{\boldsymbol{x}}_k = \sum_{i=1}^{n} \frac{\partial \boldsymbol{x}_k}{\partial q_i} \dot{q}_i + \frac{\partial \boldsymbol{x}_k}{\partial t} \tag{2}$$

The forces exerted on the kth particle can be grouped as the applied force $\boldsymbol{F}_k$ and the constraint force $\boldsymbol{R}_k$. When the constraints are workless, the Virtual Work Principle is stated as

$$\sum_{k=1}^{N} (\boldsymbol{F}_k - m_k \ddot{\boldsymbol{x}}_k)^T \delta \boldsymbol{x}_k = 0 \tag{3}$$

where $\delta \boldsymbol{x}_k$ indicates the kth virtual displacement vector. Using the generalized virtual displacement identity and generalized force definition

$$\delta \boldsymbol{x}_k = \sum_{i=1}^{n} \left(\frac{\partial \boldsymbol{x}_k}{\partial q_i} \right) \delta q_i \tag{4}$$

$$Q_i = \sum_{k=1}^{N} \boldsymbol{F}_k^T \frac{\partial \boldsymbol{x}_k}{\partial q_i} \tag{5}$$

Eq. (3) can be rewritten as

$$\sum_{i=1}^{n} \left(Q_i - \sum_{k=1}^{N} m_k \ddot{\boldsymbol{x}}_k^T \frac{\partial \boldsymbol{x}_k}{\partial q_i} \right) \delta q_i = 0 \tag{6}$$

For the general case, suppose that the system has m nonholonomic constraints given as

$$\sum_{i=1}^{n} a_{ji} \delta q_i = 0 \qquad (j = 1,2,\ldots,m)$$

then by using Lagrange multipliers λ_j, Eq. (6) can be written as

$$\sum_{i=1}^{n} \left(Q_i + \sum_{j=1}^{m} \lambda_j a_{ji} - \sum_{k=1}^{N} m_k \ddot{\boldsymbol{x}}_k^T \frac{\partial \boldsymbol{x}_k}{\partial q_i} \right) \delta q_i = 0 \tag{7}$$

and we get

$$\sum_{k=1}^{N} m_k \ddot{\boldsymbol{x}}_k^T \frac{\partial \boldsymbol{x}_k}{\partial q_i} = Q_i + \sum_{j=1}^{m} \lambda_j a_{ji} \qquad (i = 1,2,\ldots,n) \tag{8}$$

Received Sept. 4, 1990; revision received Oct. 26, 1990; accepted for publication Oct. 26, 1990.

*Gradate Student, Department of Aerospace Engineering.

†Associate Professor, Department of Aerospace Engineering. Senior Member AIAA.

‡Epright Professor, Department of Aerospace Engineering. Fellow AIAA.